

**A STUDY OF PURITY AND RECOVERY OF CARBON  
DIOXIDE FROM BINARY SYNGAS MIXTURE USING  
HYDROTALCITE IN PRESSURE EQUALIZED  
PRESSURE SWING ADSORPTION**

**NUR ASMIRA BINTI AMERNUDIN**

**UNIVERSITI SAINS MALAYSIA**

**2017**

**A STUDY OF PURITY AND RECOVERY OF CARBON  
DIOXIDE FROM BINARY SYNGAS MIXTURE USING  
HYDROTALCITE IN PRESSURE EQUALIZED  
PRESSURE SWING ADSORPTION**

by

**NUR ASMIRA BINTI AMERNUDIN**

**Thesis submitted in partial fulfilment of the requirement  
for the degree of Bachelor of Chemical Engineering**

**June 2017**

## ACKNOWLEDGEMENT

First and foremost, I would like to convey my sincere gratitude to my supervisor, Dr. Prof. Dr. Mohd Roslee Othman for his precious encouragement, guidance and generous support throughout this work.

Next, I would like to acknowledge Dr. Iliya Idris for always helping me along the research period and reaching out whenever I faced problems in experiment and writing. Her willingness to share her knowledge and spending her precious time for me to complete this research will always be appreciated and remembered.

The following person that I want to say thank you is my family who keep on supporting me and cheering me up whenever I am feeling down.

I would also extend my gratitude towards all my colleagues for their kindness cooperation and helping hands in guiding me carrying out the lab experiment. They are willing to sacrifice their time in guiding and helping me throughout the experiment besides sharing their valuable knowledge.

Apart from that, I would also like to thank all SCE staffs for their kindness cooperation and helping hands. Indeed their willingness in sharing ideas, knowledge and skills are deeply appreciated.

Once again, I would like to thank all the people, including those whom I might have missed out and my friends who have helped me directly or indirectly. Their contributions are very much appreciated. Thank you very much.

## TABLE OF CONTENT

ACKNOWLEDGEMENT	iii
TABLE OF CONTENT	iv
LIST OF TABLES	vi
LIST OF FIGURES	vii
LIST OF SYMBOLS	ix
LIST OF ABBREVIATIONS	x
ABSTRAK	xi
ABSTRACT	xii
CHAPTER ONE: INTRODUCTION	1
1.1 Research background	1
1.2 Problem statement	2
1.3 Research objective	4
1.4 Organization of thesis	5
CHAPTER TWO: LITERATURE REVIEW	6
2.1 Carbon dioxide	6
2.2 Adsorbent	7
2.3 Pressure Swing Adsorption	10
CHAPTER THREE: METHODOLOGY	12
3.1 Introduction	12
3.2 Chemicals	13

3.3 Adsorbent preparation	13
3.4 Adsorbent characterization	14
3.5 Breakthrough study	16
3.6 PSA Procedure	19
3.7 Calculation	20
CHAPTER FOUR: RESULT AND DISCUSSION	21
4.1 Characterization of HT	21
4.2 Breakthrough Analysis	28
4.3 PSA	34
CHAPTER FIVE: CONCLUSIONS AND RECOMMENDATIONS	45
5.1 Conclusions	45
5.2 Recommendations	46
REFERENCES	47
APPENDICES	55

## LIST OF TABLES

		Page
Table 2.1	List of adsorbents used in PSA research and their the results	8
Table 2.2	Comparison of previous research using pressure swing adsorption	11
Table 3.1	List of Chemicals	13
Table 4.1	Textural characteristic	22
Table 4.2	Proximate analysis of HT RAW and HT 700	27
Table 4.3	Crystallite size and lattice strain of adsorbent	28
Table 4.4	Summary of breakthrough an and saturated time of CO <sub>2</sub>	34
Table 4.5	Summary of breakthrough an and saturated time of CO <sub>2</sub>	34
Table 4.6	Operating parameter for PSA at ambient temperature	44
Table 4.7	Summary of purity and recovery of CO <sub>2</sub> using HT RAW	45
Table 4.8	Summary of purity and recovery of CO <sub>2</sub> using HT 700	45

## LIST OF FIGURES

	Page	
Figure 1.1	The rise of carbon dioxide concentration in atmosphere	4
Figure 3.1	Flowchart of experiment	12
Figure 3.2	Micromeritics ASAP 2020	14
Figure 3.3	Quantra FEG 450	15
Figure 3.4	Perkin Elmer TGA 7	15
Figure 3.5	XRD D8	16
Figure 3.6	Breakthrough analysis rig set-up	18
Figure 3.7	Rig set-up of PSA	21
Figure 4.1	Adsorption curve of HT RAW	23
Figure 4.2	Adsorption curve of HT 700	23
Figure 4.3	SEM micrographs of HT RAW at 5K magnification	24
Figure 4.4	SEM micrographs of HT RAW at 10K magnification	25
Figure 4.5	SEM micrographs of HT RAW at 30K magnification	25
Figure 4.6	SEM micrographs of HT 700 at 5K magnification	26
Figure 4.7	SEM micrographs of HT 700 at 10K magnification	26
Figure 4.8	SEM micrographs of HT 700 at 20K magnification	27
Figure 4.9	XRD pattern of HT RAW and HT 700	28
Figure 4.10	Breakthrough curve of HT RAW for CO <sub>2</sub> on different ratio	30
Figure 4.11	Breakthrough curve of HT RAW for H <sub>2</sub> on different ratio	31
Figure 4.12	Breakthrough curve of HT 700 for CO <sub>2</sub> on different ratio	32
Figure 4.13	Breakthrough curve of HT 700 for H <sub>2</sub> on different ratio	33
Figure 4.14	Purity of CO <sub>2</sub> at column 1 for HT RAW	36
Figure 4.15	Purity of CO <sub>2</sub> at column 2 for HT RAW	36

Figure 4.16	Recovery of CO <sub>2</sub> at column 1 for HT RAW	38
Figure 4.17	Recovery of CO <sub>2</sub> at column 2 for HT RAW	38
Figure 4.18	Purity of CO <sub>2</sub> at column 1 for HT 700	39
Figure 4.19	Purity of CO <sub>2</sub> at column 2 for HT 700	40
Figure 4.20	Recovery of CO <sub>2</sub> at column 1 for HT 700	41
Figure 4.21	Recovery of CO <sub>2</sub> at column 2 for HT 700	41
Figure 4.22	Purity vs recovery of CO <sub>2</sub> at 50vol% CO <sub>2</sub>	43
Figure 4.23	Purity vs recovery of CO <sub>2</sub> at 40vol% CO <sub>2</sub>	43
Figure 4.24	Purity vs recovery of CO <sub>2</sub> at 20vol% CO <sub>2</sub>	44



## LIST OF SYMBOLS

<i>m</i>	Mass flowrate	cm <sup>3</sup> /s
<i>P</i>	Pressure	bar
<i>T</i>	Time	minute
<i>W</i>	Mass of adsorbent	g

## LIST OF ABBREVIATIONS

BET	Brunauer–Emmett–Teller
CO <sub>2</sub>	Carbon dioxide
H <sub>2</sub>	Hydrogen
HT	Hydrotalcite
HT 700	Hydrotalcite calcined at 700°C
HT RAW	Raw Hydrotalcite
PSA	Pressure Swing Adsorption
SEM	Scanning Electron Microscopy
TGA	Thermogravimetric Analyser
XRD	X-Ray Powder Diffraction

**KAJIAN TENTANG KETULENAN DAN PEMULIHAN KARBON  
DIOKSIDA DAN HIDROGEN DARI CAMPURAN DEDUA GAS SINTESIS  
MENGUNAKAN HYDROTALCITE DALAM PENJERAPAN BUAI**

**TEKANAN**

**ABSTRAK**

Karbon dioksida dikenal pasti punca utama untuk kesan rumah hijau yang menghasilkan pemanasan global dan perubahan iklim. Pada hari ini, rancangan utama adalah untuk mengurangkan pengeluaran karbon dioksida. Untuk penjerap, *hydrotalcite* telah digunakan berbanding mangkin lain kerana dua factor utama yang melibatkan kos dan kadar toleransi penjerap terhadap suhu tinggi. *Hydrotalcite* lebih efektif kerana harganya yang lebih murah berbanding dengan penjerap yang lain. *Hydrotalcite* telah melalui proses pengkalsinan di suhu 700°C untuk mengkaji reaksi penjerap selepas terdedah kepada haba pada satu jangka masa. Keberkesanan penjerap untuk proses penyerapan diukur melalui analisa pemecahan di mana tempoh proses penjerapan diperolehi. Seterusnya, proses penjerapan buai tekanan dilakukan untuk mengkaji bilangan kitaran yang diperlukan sebelum penjerap menjadi tepu. Dari proses penjerapan buai tekanan ini, ketulenan dan pemulihan karbon dioksida dapat diperolehi. Kadar tertinggi diperolehi oleh HT RAW untuk ketulenan karbon dioksida ialah 84.14% dan kadar pemulihan karbon dioksida ialah 94.44%. Dari kajian ini, HT RAW boleh dikonklusikan sebagai lebih sesuai daripada *hydrotalcite* dikalsin untuk proses penjerapan buai tekanan.

**A STUDY OF PURITY AND RECOVERY OF CARBON DIOXIDE FROM  
BINARY SYNGAS MIXTURE USING HYDROTALCITE IN PRESSURE  
EQUALIZED PRESSURE SWING ADSORPTION**

**ABSTRACT**

Carbon dioxide is regarded as the main contributor to the atmospheric greenhouse effect, resulting in global warming and climate change. To reduce the emission of carbon dioxide is a major task nowadays. For the adsorption, hydrotalcite adsorption is used rather than other commercial catalyst due to two major reasons, that is related to cost and adsorbent tolerance to high temperature. Hydrotalcite is more cost effective since the price is cheaper to other adsorbent. The hydrotalcite is calcined to 700°C to see the performance of the adsorbent after being exposed to heat for a period of time. The efficiency of the adsorbent for adsorption is measured through breakthrough analysis where the adsorption length is obtained. Next, pressure swing adsorption process is run to see how much cycle is needed for the adsorbent to be exhausted. From pressure swing adsorption, the purity and recovery of carbon dioxide were obtained. The highest carbon dioxide purity achieved is 84.14% and 94.44% carbon dioxide recovery by HT RAW. From this research, it can be concluded that HT RAW is better than calcined hydrotalcite for pressure swing adsorption process.

# CHAPTER ONE

## INTRODUCTION

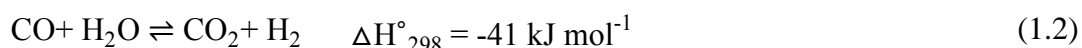
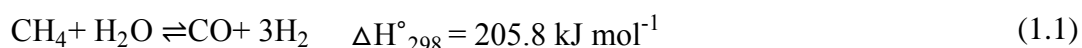
### 1.1 Research background

Global warming is getting more serious in recent years. The atmospheric concentration of carbon dioxide (CO<sub>2</sub>) has recently passed the 400ppm milestone (Kahn, 2016). CO<sub>2</sub> is mainly responsible for the atmospheric greenhouse effect, which is causing the warming of the climate system. It is extremely likely that human influence has been the dominant cause of the observed warming (Riboldi and Bolland, 2015b). To reduce the emission of CO<sub>2</sub> is a major task nowadays. This research studies the separation of carbon dioxide from syngas by pressure swing adsorption (PSA) process, so that the concentrated carbon dioxide can be captured to reduce the greenhouse effect (Chou et al., 2016). A pressure swing adsorption (PSA) process is to separate high-purity hydrogen (H<sub>2</sub>) and to capture CO<sub>2</sub> from synthesis gas, which is the effluent stream of a water-gas-shift reactor. The purified H<sub>2</sub> can be sent to a gas turbine to generate electrical power or can be used for other energy sources, whilst the CO<sub>2</sub> can be recovered and sequestered to reduce greenhouse-gas effects (Chou et al., 2013). Pressure swing adsorption processes are believed to be a promising option for achieving more energy and cost-effective capture of CO<sub>2</sub> from large point sources, especially coal-fired power plants (Riboldi et al., 2014). Pressure swing adsorption uses cyclic pressure swing process to separate gas mixture, according to the difference of adsorption capacity of adsorbent due to different pressure (Chou et al., 2016). The adsorption column (bed) is packed with adsorbent. Adsorbents play a key role in adsorption technology. The adsorbent determines the overall CO<sub>2</sub> capture performance in PSA technology. The key elements for a good adsorbent in CO<sub>2</sub> PSA technology

are high selectivity of CO<sub>2</sub> over H<sub>2</sub>, high adsorption capacity of CO<sub>2</sub>, rapid adsorption/desorption kinetics, stable adsorption capacity after repeated cycles, and adequate mechanical strength of the particles (Ling et al., 2014). The main application of this work is to determine the purity and recovery of CO<sub>2</sub>/H<sub>2</sub> by using HT as the adsorbent in the PSA.

## 1.2 Problem statement

Syngas, a mixture of hydrogen and carbon monoxide, plays a significant role in both chemical and petrochemical industries (Omogbe et al., 2017). Syngas has been widely utilized as the main feedstock for producing eco-friendly synthetic fuels and methanol through Fischer-Tropsch synthesis and methanol production (Borg et al., 2007, Vo and Adesina, 2012, Olah et al., 2015, Omogbe et al., 2017). Syngas can be produced by various methods such as coal gasification, partial oxidation and steam reforming of methane (Yoon and Lee, 2012, Pantaleo et al., 2016, Salhi et al., 2011, Arcotumapathy et al., 2014, Omogbe et al., 2017). Among other options, this research focuses on production of syngas from steam reforming of methane as it is the most cost effective method (Salhi et al., 2011).



Carbon deposit can also be formed through Boudouart reaction and/or methane decomposition (Salhi et al., 2011).



Nonetheless, the precise formulation is varied due to the need for carbon deposition control and minimization along with the procurement of high catalyst activity, product

selectivity and stability (Arcotumapathy et al., 2014). Nevertheless, emission of greenhouse gases particularly carbon dioxide, which greatly contribute to global warming, is the major drawback of all these processes (Curtis, 2009, Bradford and Vannice, 1999, Omoregbe et al., 2017). The drastic increase of carbon dioxide concentration in the atmosphere is quite worrying. Based on statistic, carbon dioxide concentration in 2013 had surpassed 400ppm for the first time in centuries as shown in Figure 1.1 below (Shaftel, 2017c). The rise in carbon dioxide concentration will eventually contribute to the climate change, which is the main cause of global warming to taking place. Global warming happens due to the greenhouse effect when the atmosphere traps heat that is being radiated from the earth into space (Shaftel, 2017a). The consequence of global warming is causing the earth to become warmer. Warmer earth will contribute to the melting of ice in the Greenland and Antarctic that will also contribute to the rise of sea level (Shaftel, 2017b). Moreover, the increasing carbon dioxide in the atmosphere will also cause the ocean acidification. This happens when more carbon dioxide is being absorbed into the ocean (Shaftel, 2017b). As mention on the earlier part of this section, carbon dioxide is part of syngas. The high production of syngas will also lead to high carbon dioxide emission to the atmosphere. Thus, it became a big concern on separating carbon dioxide from the syngas. Therefore, this research is one of the ways to solve this excessive carbon dioxide emission to the atmosphere by using pressure swing adsorption (PSA). PSA is a cyclic process based on the capability of some solid adsorbents to selectively attract carbon dioxide molecules on their surface. Feed is stopped before the adsorbent bed becomes saturated. Next, a regeneration process is performed by reducing the total pressure of the whole PSA system. PSA has been considered in this research for its potential low energy requirements (Riboldi and Bolland, 2015a).

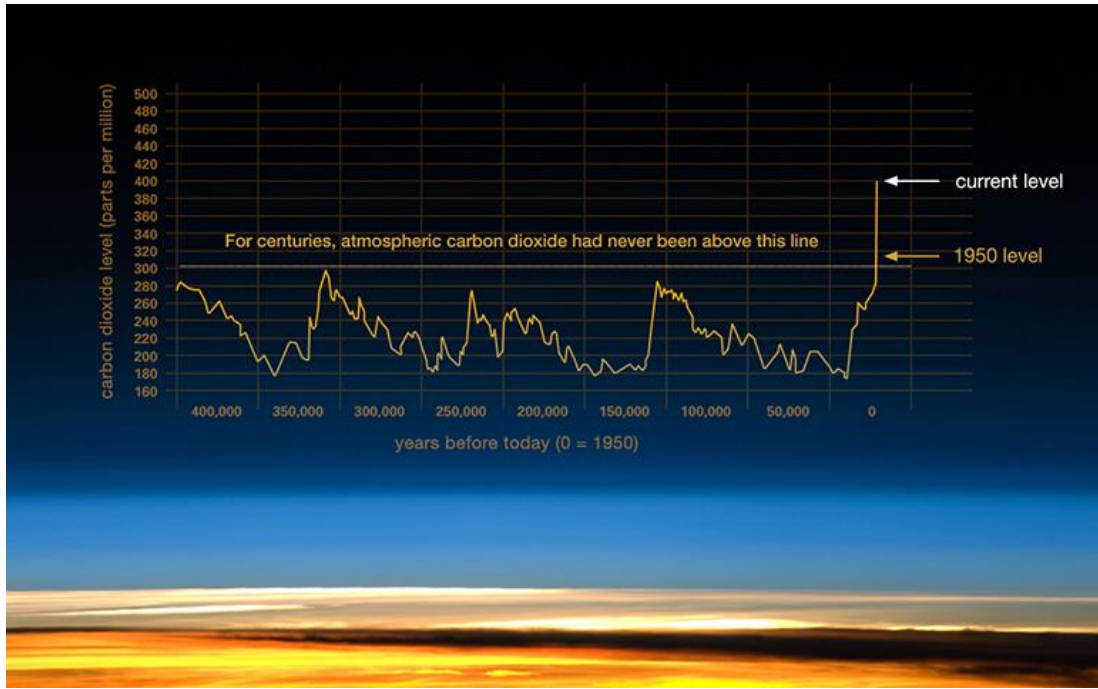


Figure 2.1 The rise of carbon dioxide concentration in atmosphere (Shaftel, 2017c)

### 1.3 Research objective

The aims of this research research are:

1. To prepare and characterize the raw Hydrotalcite and calcined Hydrotalcite as the adsorbents.
2. To evaluate the effect on breakthrough study by varying gas composition and adsorbent.
3. To evaluate the effect of the operating condition on purity and recovery using pressure swing adsorption.



## 1.4 Organization of thesis

This thesis consists of five main chapters and each chapter contributes to the sequence of this study. The following are the contents for each chapter in this study:

1. **Chapter 1** introduces the properties of syngas and the effects of carbon dioxide on the environment, problem statement, research objectives, scope of study and organization of thesis.
2. **Chapter 2** discusses the literature review of this study. An insight into carbon dioxide, adsorbent and vacuum pressure swing adsorption.
3. **Chapter 3** covers the experimental work conducted. This includes the list of chemicals, adsorbent preparation, catalyst characterization, experimental set-up and experimental procedures.
4. **Chapter 4** refers to the experimental results and discussions of the data obtained. Further elaboration on characterization of adsorbent, breakthrough analysis and data obtained from the PSA experiment.
5. **Chapter 5** concludes all the findings obtained in this study. Recommendations are also included as well.

## **CHAPTER TWO**

### **LITERATURE REVIEW**

#### **2.1 Carbon dioxide**

Carbon dioxide (CO<sub>2</sub>) emissions, mainly caused by humans, increased from 21 giga tons per year to 38 giga tons per year since 1970 (Rammerstorfer and Eisl, 2011). The largest source of CO<sub>2</sub> emissions is from the consumption of fossil fuels. Fossil fuels represent more than 80% of the world energy portfolio and 95% of our organic-based chemicals rely on non-renewable resources, such as hydrocarbons, which make greenhouse gas emissions to reaching alarming rates (Olajire, 2013). As fossil fuel is non-renewable and is a limited resources, whenever carbon is remove from the ground in the form of coal, natural gas, and oil, it is transferred to the atmosphere in the form of CO<sub>2</sub> (Saric et al., 2016). The atmosphere will continue to contain the rising quantities of carbon as CO<sub>2</sub> while fossil fuels diminished in supply (Saric et al., 2016). The increased in CO<sub>2</sub> concentration has led to increasing in global temperatures and critical changes to the climate, mainly within the past few decades (Saric et al., 2016). The 2015–16 El Nino event has recorded high CO<sub>2</sub> concentration at the Mauna Loa observatory such that the annual mean CO<sub>2</sub> concentration is predicted to remain above 400 ppm into the future (Saric et al., 2016). Therefore, it will be beneficial to find sustainable methods of converting atmospheric or captured waste-stream CO<sub>2</sub> into usable fuels (Saric et al., 2016, Olajire, 2013). During this process, CO<sub>2</sub> is removed from the flue gases of large emitters, such as power plants, via membrane separation or an absorbent/adsorbent which then the captured CO<sub>2</sub> will be stored either in deep ocean or underground in geological formations such as depleted oil and gas reservoirs (Olajire, 2013). The overall holding capacity for CO<sub>2</sub> storage is estimated to reach

between 2000giga tons and 11,000giga tons, worldwide (Rammerstorfer and Eisl, 2011). As stated in Chapter One, CO<sub>2</sub> is generated from the steam reforming of methane and its end product is syngas. Syngas composition can be varied depending on the feedstock, however the typical composition is 30% to 60% carbon monoxide, 25% to 30% hydrogen, 0% to 5% methane, 5% to 15% carbon dioxide, plus a lesser or greater amount of water vapor, smaller amounts of the sulfur compounds hydrogen sulfide, carbonyl sulfide and finally some ammonia and other trace contaminants (Laboratory, 2017).

## **2.2 Adsorbent**

An adsorbent is a solid substance used to adsorb solute molecules from a liquid or gas. Adsorbent is widely used in adsorption process along with membrane. There is a variety of adsorbents and each has its own unique feature to suit with the condition of the research. Table 2.1 shows the results of research done by researchers who use a variety of adsorbent to adsorb many types of gases.

Table 2.1 List of adsorbents used in PSA research and their the results

<b>Adsorbent</b>	<b>Type of Feed Gas</b>	<b>Feed Gas Composition</b>	<b>Result Details</b>	<b>References</b>
Silica gel	Flue gas	85% N <sub>2</sub> , 15% CO <sub>2</sub>	90.77% CO <sub>2</sub> purity, 76.47% CO <sub>2</sub> recovery	(Yan et al., 2016)
Zeochem Zeolite 13X	Flue gas	85% N <sub>2</sub> , 15% CO <sub>2</sub>	94.861% CO <sub>2</sub> purity, 89.765.6% CO <sub>2</sub> recovery	(Krishnamurthy et al., 2014)
AC5-KS	Syn gas	1.3% CO, 41.4% CO <sub>2</sub> , 57.3% H <sub>2</sub>	92% CO <sub>2</sub> purity, 98% CO <sub>2</sub> recovery	(Chou et al., 2013)
Activated Carbon	Syn gas	0.380% CO <sub>2</sub> , 0.537% H <sub>2</sub> , 0.016% CO, 0.067% N <sub>2</sub>	85.3% CO <sub>2</sub> purity, 88.7% CO <sub>2</sub> recovery	(Riboldi and Bolland, 2015a)
Hydrotalcite	Syn gas	21.5% CO <sub>2</sub> , 16.8% H <sub>2</sub> O and remainder N <sub>2</sub> / H <sub>2</sub>	97.2% CO <sub>2</sub> purity, 94.8% CO <sub>2</sub> recovery	(Xiao et al., 2009)

### 2.2.1 Hydrotalcite

The type of adsorbent used in this research is hydrotalcite(HT) which is also known as layered double hydroxide in which divalent cations within brucite-like layers are replaced by trivalent cations (Wiyantoko et al., 2015, Isa et al., 2008, Yang et al., 2005, Wang et al., 2012). The resulting positive charge is compensated by hydrated anions located in the interlayer space between two brucite sheets (Yang et al., 2005,

Wiyantoko et al., 2015). HT is extensively used as anion exchangers, adsorbents, catalysts and catalyst supports, and additives to plastics (Wiyantoko et al., 2015, Yang et al., 2005, Wang et al., 2012). HT are usually chosen over other compounds due to the versatility, simplicity, easily tailored properties and low cost of the materials (Othman et al., 2009, Low, 2011). HT possesses capabilities to separate carbon dioxide by means of adsorption because of high abrasion resistance, high thermal stability and small micropore diameter, which results in higher capacity of adsorption and stable interdispersion of the active species with high reproducibility (Isa et al., 2008, Abelló and Pérez-Ramírez, 2006, Albertazzi et al., 2007). In this research, a raw hydrotalcite (HT RAW) powder obtained commercially was used as an adsorbent. The HT was calcined to 600°C, 700°C and 800°C to observe the effectiveness of each calcined adsorbent in adsorbing carbon dioxide. When HT is being calcined around 500°C, the decomposition of HT leads to mixed metal oxides, which are characterized by high specific surface areas and homogeneous dispersion of metal cations (Li et al., 2008). The mixed metal oxides can rehydrate and combine with anions from aqueous solutions to reconstruct the original structure (Li et al., 2008). Therefore, it strengthens the statement which states that calcined HT has the potential as an ion exchanger/adsorbent for removal of toxic anions from contaminated water (Li et al., 2008, Das et al., 2003, Orthman et al., 2003, Das et al., 2004). The purpose of using hydrotalcite in this research is because of its ability to withstand high temperature. In real life industry, steam reforming of methane took place at high temperature, about 900°C. Therefore, the adsorbent used to capture CO<sub>2</sub> needs to be able to work moderately at about 300°C-500°C (Yang and Kim, 2006). Moreover, hydrotalcite is being reported to have good features of adsorbents for CO<sub>2</sub> adsorption at high temperatures since it has magnesium-aluminum containing layered double hydroxides

(LDH) (Yang and Kim, 2006, Hufton et al., 1999, Yong et al., 2001). For that reason, hydrotalcite is suitable for this research.

### **2.3 Pressure Swing Adsorption**

There is a variety of CO<sub>2</sub> capture technologies. It is either physical absorption, chemical absorption, adsorption or membrane (Dave et al., 2016, Dinca et al., 2017, Ribeiro et al., 2011, Dai and Deng, 2016, Ribeiro et al., 2010). In this research, adsorption process is used to capture CO<sub>2</sub>, pressure swing adsorption (PSA) to be more precise. PSA technology has proven to be a more an economical alternative to such systems for the purification of H<sub>2</sub> obtained by steam reforming (Ribeiro et al., 2011). The objective of the PSA process is to separate the CO<sub>2</sub> from the feed mixture and produce it with purity above 95% (Ribeiro et al., 2011). Between all methods of CO<sub>2</sub> capturing, PSA looks promising due to the constitutionally low energy consumption, low capital cost, and safety and simplicity of operation (Schell et al., 2013, Augelletti et al., 2017).

Table 2. show a comparison of previous research done on capturing CO<sub>2</sub> by using PSA. Besides PSA, temperature swing adsorption is also used to capture carbon dioxide. In PSA, the adsorption step is performed at atmospheric pressure and desorption is obtained under low pressure (Zhao et al., 2017). Meanwhile, for temperature swing adsorption, the column is heated by a feed of hot gas or steam, and the following step is the cooling of the adsorption bed by a feed of cold gas before next adsorption cycle (Zhao et al., 2017).

Table 2.2 Comparison of previous research using pressure swing adsorption

<b>Adsorbent</b>	<b>Pressure Range (kPa)</b>	<b>Feed Gas Composition</b>	<b>Result Details</b>	<b>References</b>
Activated Carbon	2500 - 3400	40% CO <sub>2</sub> , 60% H <sub>2</sub>	95% CO <sub>2</sub> purity, 95% CO <sub>2</sub> recovery	(Casas et al., 2013)
Activated Carbon	3880	53.5% H <sub>2</sub> , 37.9% CO <sub>2</sub> , 1.5% CO, 0.06% CH <sub>4</sub> , 6.7% N <sub>2</sub> , 0.3% Ar, 0.0001% H <sub>2</sub> S, 0.03% H <sub>2</sub> O	98.9% CO <sub>2</sub> purity, 86.1% CO <sub>2</sub> recovery	(Riboldi and Bolland, 2015b)
Zeolite 5A	3880	53.54% H <sub>2</sub> , 37.89% CO <sub>2</sub> , 1.5% CO, 0.06% CH <sub>4</sub> , 6.72% N <sub>2</sub> , 0.27% Ar, 0.0001% H <sub>2</sub> S, 0.03% H <sub>2</sub> O	98.9% CO <sub>2</sub> purity, 89.7% CO <sub>2</sub> recovery	(Riboldi et al., 2014)
Zeolite 13X	450.896	41.4% CO <sub>2</sub> , 1.3% CO, 57.3% H <sub>2</sub>	96.95% CO <sub>2</sub> purity, 96.6% CO <sub>2</sub> recovery	(Chou et al., 2016)
Hydrotalcite	2700	21.5% CO <sub>2</sub> , 16.8% H <sub>2</sub> O and remainder N <sub>2</sub> / H <sub>2</sub>	97.2% CO <sub>2</sub> purity, 94.8% CO <sub>2</sub> recovery	(Xiao et al., 2009)
A Promoted Hydrotalcite-Based Material	2360	32.6% H <sub>2</sub> O, 34.6% H <sub>2</sub> , 4.7% CO, 23.8% CO <sub>2</sub>	98% CO <sub>2</sub> purity, 90% CO <sub>2</sub> recovery	(Reijers et al., 2011)

## CHAPTER THREE

### METHODOLOGY

#### 3.1 Introduction

This chapter describes all the experimental work conducted. This includes the list of chemicals, adsorbent preparation, catalyst characterization, experimental set-up and experimental procedures as shown in Figure 3.1.

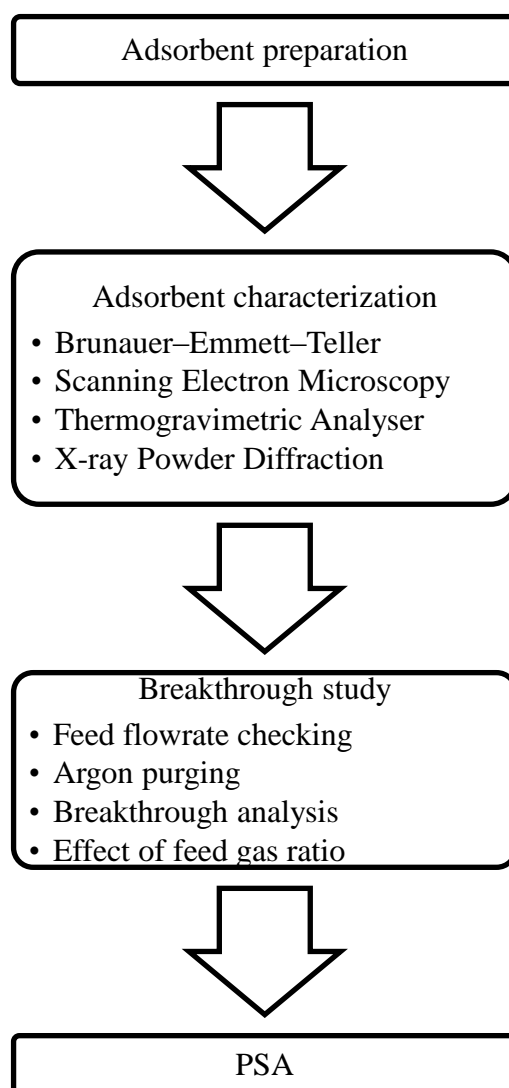


Figure 3.1 Flowchart of experiment



### 3.2 Chemicals

Table 3.1 shows the chemicals involved in the preparation of HT.

Table 3.1 List of Chemicals

Chemicals	Purpose	Supplier
Aluminium nitrate nonahydrate, $\text{Al}(\text{NO}_3)_3 \cdot 9\text{H}_2\text{O}$	Metal oxide precursor	Merck
Magnesium nitrate hexahydrate, $\text{Mg}(\text{NO}_3)_2 \cdot 9\text{H}_2\text{O}$	Metal oxide precursor	Merck
Sodium carbonate, $\text{Na}_2\text{CO}_3$	Anions for charge balancing	Merck
Poly (vinyl-alcohol), $(\text{C}_2\text{H}_4\text{O})_n$	Binder	Merck
Glycine, $\text{H}_2\text{NCH}_2\text{COOH}$	Combustive fuel	Merck
Deionized water, $\text{H}_2\text{O}$	Solvent	N/A

### 3.3 Adsorbent preparation

20g of  $(\text{Mg}(\text{NO}_3)_2 \cdot 6\text{H}_2\text{O})$  and 6.67g of  $(\text{Al}(\text{NO}_3)_3 \cdot 9\text{H}_2\text{O})$  were mixed in deionized water at  $100^\circ\text{C}$  (Salleh, 2012). The mixture was stirred at a temperature  $60^\circ\text{C}$  to  $70^\circ\text{C}$ . Then 2.5g of a mixture of 0.20wt%  $\text{Na}_2\text{CO}_3$  and 4wt% Polyvinyl-alcohol were added into the mixture. The mixture was then stirred vigorously. The mixture was heated at a temperature of  $80^\circ\text{C}$  until it turns into paste. The paste was heated at  $700^\circ\text{C}$  for 5 minutes respectively. The paste now turns into Mg-Al-O. Mg-Al-O then was soaked in 1N  $\text{Na}_2\text{CO}_3$  for 5 minutes and allowed to centrifuged. Next, the powder was washed and dried.

### **3.4 Adsorbent characterization**

#### **3.4.1 Brunauer–Emmett–Teller (BET)**

Adsorbent characterization starts with the study on surface area, pore volume and pore size distribution by using BET (Shahkarami et al., 2015). The analysis was carried out using Micromeritics ASAP 2020 as shown in Figure 3.2. The BET surface area was obtained by applying BET equation to the adsorption data (Hakimi, 2015). The standard ASAP 2020 was furnished with six analysis gas inlets and a 1000-mmHg transducer for analysis of most routine samples and a line of options that can be adjusted to the needed system.



Figure 3.2 Micromeritics ASAP 2020

#### **3.4.2 Scanning Electron Microscopy (SEM)**

The analysis of the surface morphology of HT powder was done using SEM; model Quanta FEG 450 as shown in Figure 3.3 (Isa et al., 2008, Salleh, 2012). It was used to retrieve the SEM images at distinct magnification (Hakimi, 2015). SEM could also give out information on external morphology (texture), chemical composition and crystalline structure and orientation of materials making up the sample (Swapp). In addition, SEM is generally being used to analyse phases based on qualitative chemical analysis and/or crystalline structure (Swapp).



Figure 3.3 Quanta FEG 450

### 3.4.3 Thermogravimetric Analyser (TGA)

As seen in Figure 3.4, the model of TGA used for this HT characterization is Perkin Elmer TGA 7. TGA can identify and quantify loss of water, loss of solvent, loss of plasticizer, decarboxylation, pyrolysis, oxidation, decomposition, weight % filler, the amount of metallic catalytic residue remaining on carbon nanotubes, and weight % ash. All these quantifiable applications are commonly performed upon heating, but there are some experiments where information may be attained upon cooling.



Figure 3.4 Perkin Elmer TGA 7

### 3.4.4 X-Ray Powder Diffraction (XRD)

To analyse the chemical composition inside the adsorbent, XRD was used (Isa et al., 2008). The model used was Bruker D8 ADVANCE XRD as shown in Figure 3.5. This model used an X-ray tube with a copper anode as the primary X-ray beam source that emitted 8keV and 14keV X-ray with corresponding wavelengths of 1.54Å and 0.8Å, respectively (Manning and Ichimura, 2006).



Figure 3.5 XRD D8

### 3.5 Breakthrough study

The breakthrough analysis rig set-up is shown in Figure 3.7. Adsorption capacity was analysed by using the breakthrough curve in adsorption column and the bed adsorption capacity was studied as a function of both breakthrough time and the S-shape of the breakthrough curve under the designed operating conditions (Shahkarami et al., 2015). The operating condition for this experiment was varying the ratio of the feed gas and varying the type of adsorbent. The adsorption capacity was obtained from online gas chromatography, which was connected with the reactor. A graph of  $C/C_0$  against time can be plotted from the result obtained. From the result obtained, a graph of  $C/C_0$  against time was plotted.

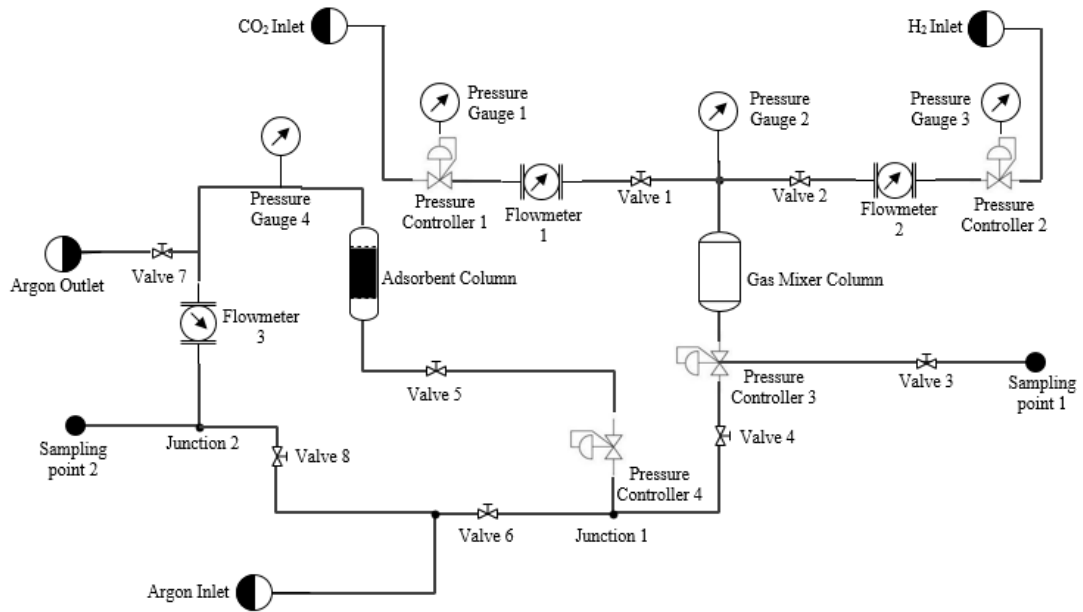


Figure 3.6 Breakthrough analysis rig set-up

### 3.5.1 Experimental procedure

#### 3.5.1.1 Feed flow rate checking

The feed gas ratio was set at the Flowmeter 1 and Flowmeter 2 for CO<sub>2</sub> gas and H<sub>2</sub> gas respectively. First, ensure that Pressure Controller 3 and 4 and Valve 1, 2, 3, 4 and 6 has been closed. The tube from Valve 4 was disconnected at the Junction 1 and the tube was connected to the Mass Flow Controller. After the Mass Flow Controller had stabilized, Pressure Controller 3 and Valve 4 were opened. Next, Valve 1 was opened. By using the Flowmeter 1, CO<sub>2</sub> gas was set up to the required flowrate. After that, Valve 1 was closed and Valve 2 was opened. By using the Flowmeter 2, H<sub>2</sub> gas was set up to the required flowrate. Valve 4 was closed and Valve 1 and 3 were opened. Connected the Sampling Point 1 to the gas chromatography to check the feed flowrate. The tube from Valve 4 was disconnected from the Mass Flow Controller and connected back to the Junction 1. After targeted feed gas ratio had been achieved, the Sampling Point 1 was disconnected from the gas chromatography.

### **3.5.1.2 Argon purging**

Firstly, ensure that Pressure Controller 4 and Valve 4, 5, 6, 7 and 8 were close. Next, the adsorbent was filled inside the adsorbent column. After that, Valve 6 was opened and followed by the opening of the Pressure Controller 4. Valve 5 was opened slowly and the Pressure Gauge 4 was checked to show the reading of 1bar. The argon gas was left to purge through the adsorbent for 30minutes. Argon purge is needed to clean the adsorbent from the atmospheric gases.

### **3.5.1.3 Breakthrough analysis**

To start the breakthrough analysis, firstly, the valve 6 was closed, followed by the closing of Valve 5. The argon gas was purged out and emptied the Adsorbent Column. If the Pressure Gauge 4 still does not give a zero reading, Valve 7 is to be opened slowly to completely purge out the argon gas. After all the argon gas had been purged out, Valve 7 was closed. The Sampling Point 1 is then disconnected from gas chromatography while Sampling Point 2 was connected to the gas chromatography. Next, Valve 4 and Pressure Controller 4 were opened. Valve 5 was opened slowly until Pressure Controller 4 showed the reading of 1bar. After that, the start button at the gas chromatography was pressed and the analysis was run for 2hours.

### **3.5.2 Effect of feed gas ratio**

There are three ratios of feed gas that are being used which are 50% CO<sub>2</sub>: 50% H<sub>2</sub>, 40% CO<sub>2</sub>: 60% H<sub>2</sub> and 20% CO<sub>2</sub>: 80% H<sub>2</sub>. The feed gas ratio was set at the Flowmeter 1 and Flowmeter 2 for CO<sub>2</sub> and H<sub>2</sub> gas respectively. Mass Flow Controller identified the flowrate of each gases. For the first ratio, 50% CO<sub>2</sub>: 50% H<sub>2</sub>, CO<sub>2</sub> gas was set up to 30ml, which was equivalent to 50% and H<sub>2</sub> gas was set up to 30ml, which was also

equivalent to 50%. For the second ratio, which was 40% CO<sub>2</sub>: 60% H<sub>2</sub> ratio, 20ml was equivalent to 40% and 30ml equivalent to 60% and for the last ratio, 20% CO<sub>2</sub>: 80% H<sub>2</sub>, 7.5ml was equivalent to 20% and 30ml equivalent to 80%.

### **3.6 PSA Procedure**

Figure 3.8 shows the rig set-up for vacuum pressure swing adsorption. The bed was filled with the adsorbent. Valve 1 and 5 were opened while valve 4 was closed to pressurize Column A to 8bar with gas from the inlet and depressurized Column B to 1bar by releasing gases inside column at Gas Outlet 1. CO<sub>2</sub> gas was adsorbed inside Column A until the adsorbent bed was saturated. Valve 7 was opened to purge out the H<sub>2</sub> gas at Gas Outlet 2. Meanwhile, at Column B, a fraction of purified H<sub>2</sub> gas was used to purge out CO<sub>2</sub> gas out of Column B to the atmosphere through Gas Outlet 1. Next is the equalization stage where the pressure in both columns was equalized to save some energy. To have same pressure inside both of columns, Valve 2 and 4 were opened while Valve 3 and 6 were closed. This process was continued until both columns have the pressure of 4bar. After 4bar had achieved in both columns, Valve 1, 3, 5 and 6 were closed while Valve 2 and 4 were opened. This was to depressurize Column A to 1bar by releasing the CO<sub>2</sub> gas to atmosphere through Gas Outlet 1 with the help of a fraction of purified H<sub>2</sub> gas. Meanwhile, Column B was pressurized until 8bar with the gas from the inlet. CO<sub>2</sub> gas was adsorbed inside Column B until the adsorbent bed was saturated. Valve 8 was opened to purge out the H<sub>2</sub> gas at Gas Outlet 2. Lastly, another equalization stage where the pressure in both columns were equalized takes place. To have the same pressure inside both of columns, Valve 2, 4 and 8 were closed while Valve 3 and 6 were opened. This process was continued until both columns had the pressure of 4bar.

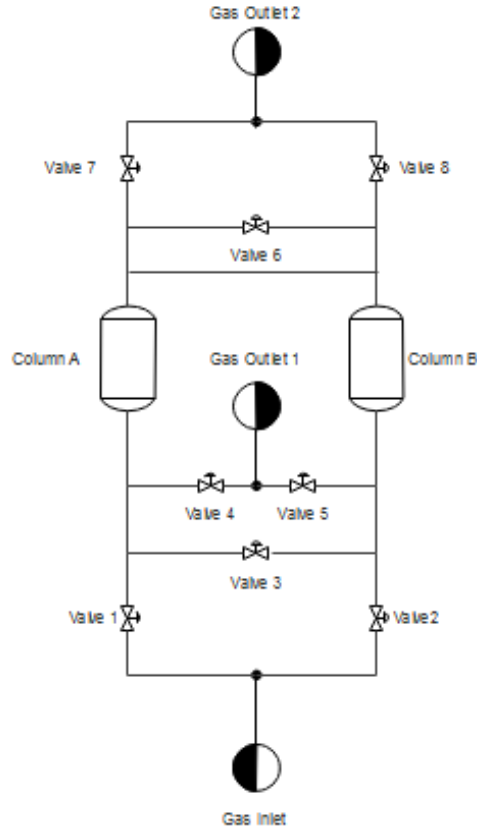


Figure 3.7 Rig set-up of PSA

### 3.7 Calculation

The results obtained from the PSA experiments were calculated using the formula below to obtain the purity and recovery of CO<sub>2</sub> and H<sub>2</sub>:

$$\text{Purity of CO}_2(\%) = \frac{\text{Amount of CO}_2 \text{ vol\% in the product stream}}{\text{Total amount of component in product stream}} \quad (3.1)$$

$$\text{Recovery of CO}_2 (\%) = \frac{\text{Amount of CO}_2 \text{ vol\% in the product stream}}{\text{Amount of CO}_2 \text{ vol\% in the feed stream}} \quad (3.2)$$

$$\text{Purity of H}_2(\%) = \frac{\text{Amount of H}_2 \text{ vol\% in the product stream}}{\text{Total amount of component in product stream}} \quad (3.3)$$

$$\text{Recovery of H}_2 (\%) = \frac{\text{Amount of H}_2 \text{ vol\% in the product stream}}{\text{Amount of H}_2 \text{ vol\% in the feed stream}} \quad (3.4)$$



## CHAPTER FOUR

### RESULTS AND DISCUSSION

#### 4.1 Characterization of HT

##### 4.1.1 BET

As illustrated in Table 4.1, the average pore diameter for HT RAW is 22nm and HT 700 is 6nm. Both adsorbents are mesopores. The decrease in average pore diameter after HT being calcined might be due to the heat treatment received by HT 700 during calcination. Figure 4.1 and Figure 4.2 showed the adsorption graph of HT Raw and HT 700 respectively. Based on the figures, both adsorption falls into Type 2 isotherm, which correlate to materials having pore diameters larger than micro-pores. Type 2 isotherm signifies an unrestricted monolayer-multilayer adsorption (Othman et al., 2017).

Table 4.1 Textural characteristic

Samples	$S_{BET}$ (m <sup>2</sup> /g)	Average pore diameter (nm)	Pore volume (cm <sup>3</sup> /g)
HT RAW	11	22	0.037588
HT 700	240	6	0.075534

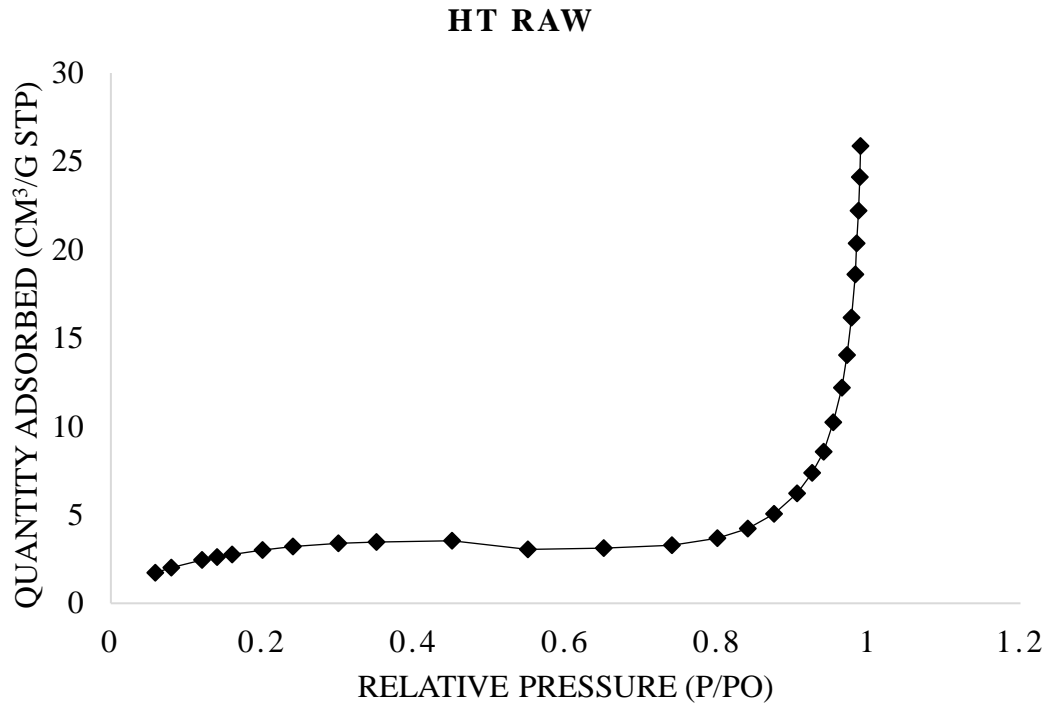


Figure 4.1 Adsorption curve of HT RAW

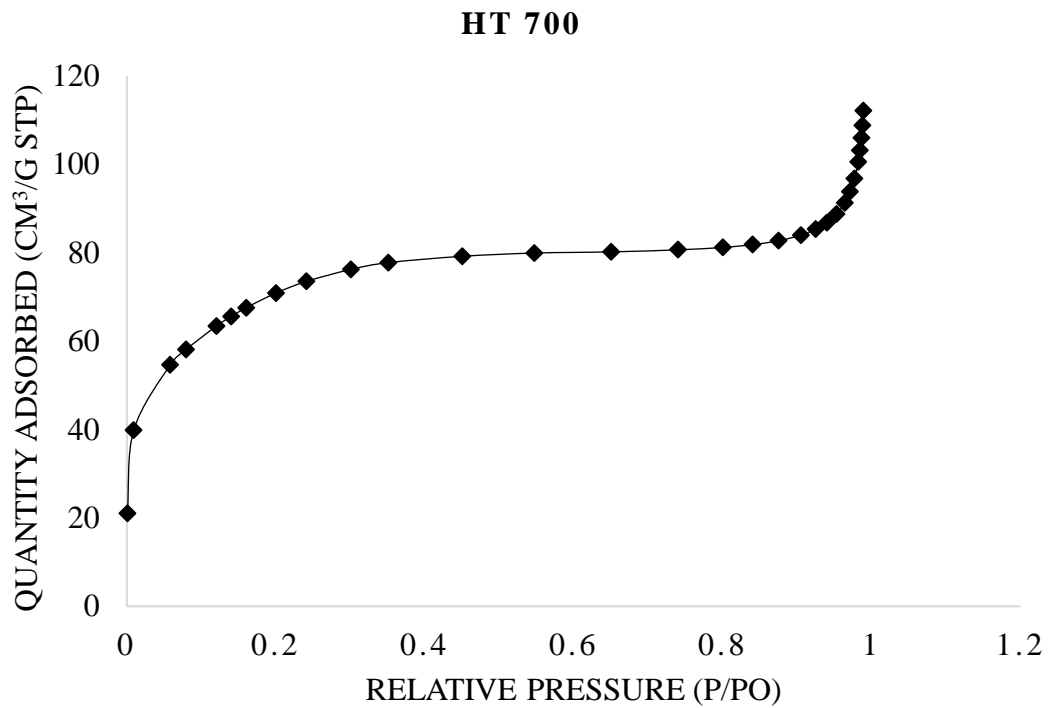


Figure 4.2 Adsorption curve of HT 700

#### 4.1.2 SEM

The textural structure of HT RAW and HT 700 was observe by SEM images as shown in Figure 4.3, Figure 4.4 and Figure 4.5 while SEM images of HT 700 can be observed in Figure 4.6, Figure 4.7 and Figure 4.8. When hydrotalcite is being exposed to mixed oxide during calcination process, the structure of the adsorbent remained the same, but the size decreasing. As stated by Xie et. al (2006) in their research, where  $Al^{3+}$  substitutes for the  $Mg^{2+}$  sites in the adsorbent and next changed to periclase-like Mg–Al–O solid solutions by calcination at a high temperature. Therefore, the morphology of hydrotalcite after calcined does not differ from the uncalcined one. By having thermal treatment, hydrotalcites managed to undergo substitution of interlayer carbonate by hydroxyl group however having no severe effect on the original ordered stacked structure of the aggregates (Xie et al., 2006).

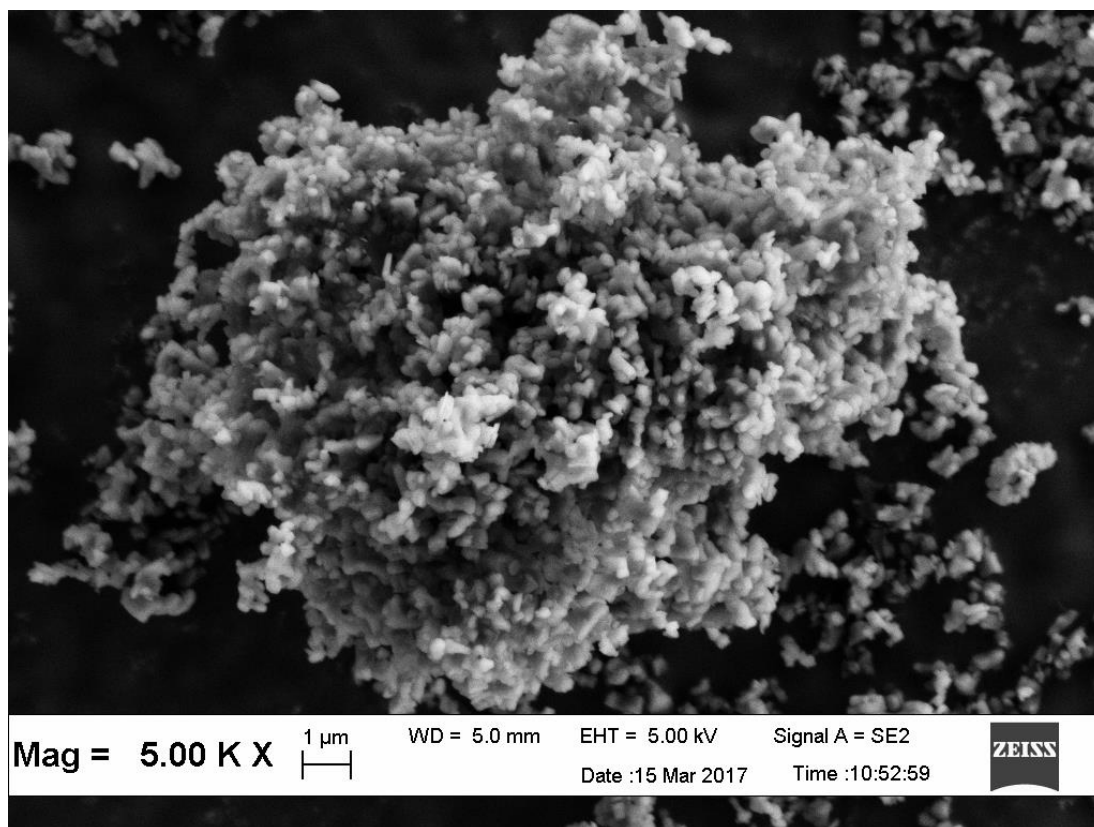


Figure 4.3 SEM micrographs of HT RAW at 5K magnification

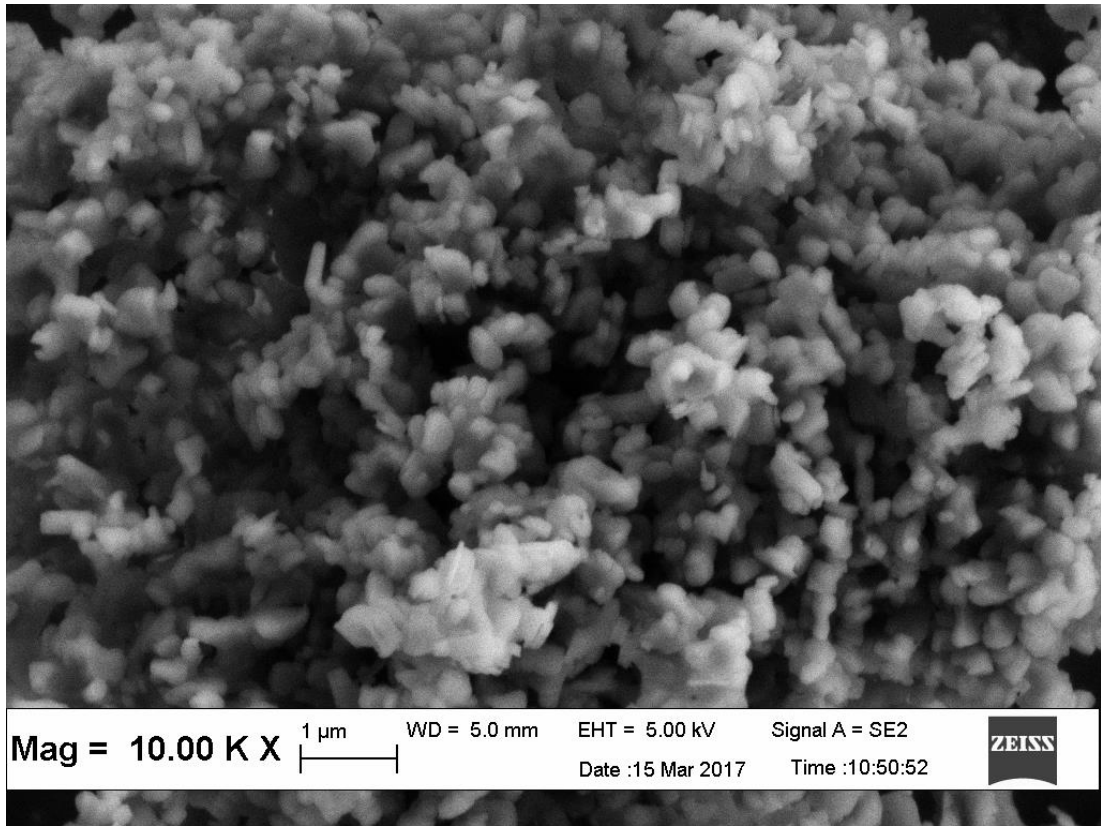


Figure 4.4 SEM micrographs of HT RAW at 10K magnification

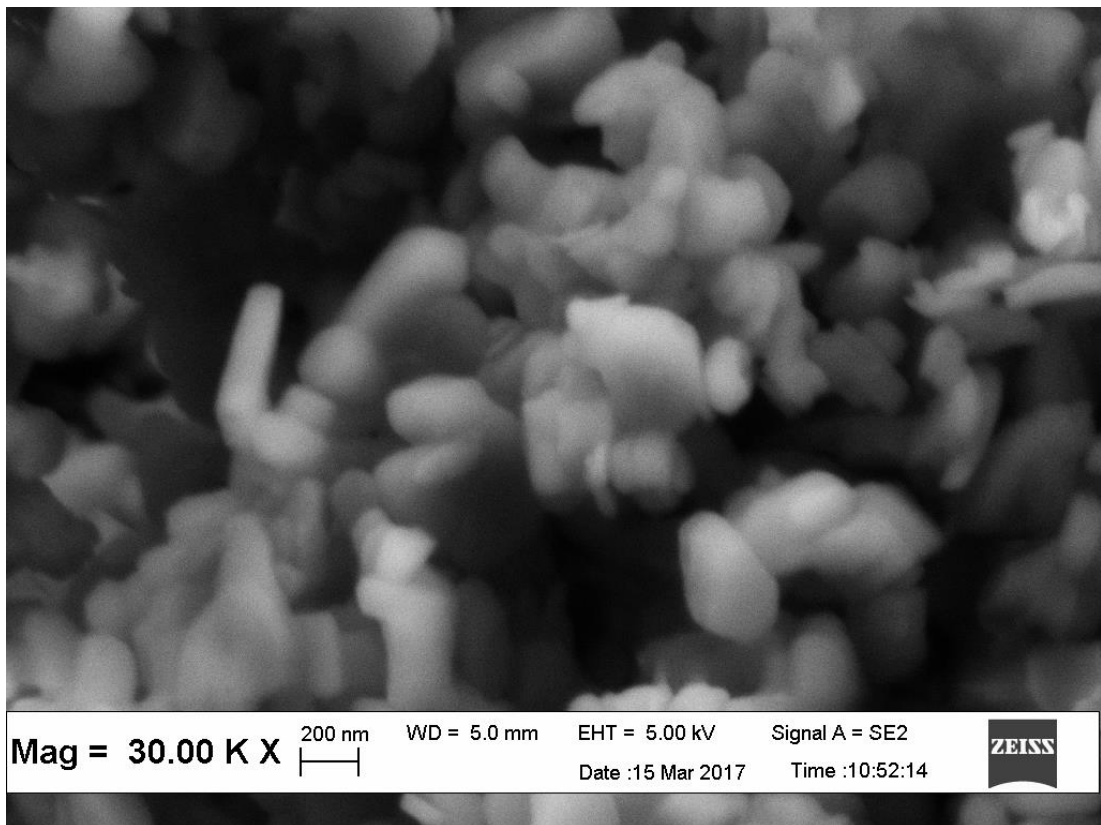


Figure 4.5 SEM micrographs of HT RAW at 30K magnification